

COASTAL WAVE MODELING FOR JETTY REHABILITATION AT COOS BAY, OREGON

Lihwa Lin¹ and Zeki Demirebelik¹

Coos Bay Inlet, located on the Pacific coast of southwestern Oregon, is protected by dual jetties constructed in 1928. Because the inlet is exposing to high energy environment, both north and south jetties have deteriorated since the initial construction. Aging, erosion of foundation, lack of effective maintenance, and channel dredging in the past have accelerated the jetty deterioration. To ensure navigation safety, the U.S. Army Corps of Engineers is presently investigating the rehabilitation and redesign of jetties. This paper is focused on numerical storm wave modeling of the existing jetties to provide input forcing information to physical model and redesign of jetties.

Keywords: numerical wave modeling, Coos Bay Inlet, jetty rehabilitation

INTRODUCTION

Coos Bay is located on the Pacific coast of southwestern Oregon, USA. The bay has a narrow V-shaped surface approximately 20 km long and 2.5 km wide with the area at mid tide around 38 square km. It connects to the Pacific Ocean through the Coos Bay Inlet with a Federal channel, authorized at 210 m wide and 14.3 m deep, protected by dual jetties constructed in 1928. Because the inlet is exposing to high energy Pacific coast and surrounding with strong tidal dynamics, both north and south jetties have deteriorated since their initial construction. Aging, erosion of foundation, lack of adequate maintenance, and channel deepening and dredging projects in the past also expedited the jetty deterioration. To ensure navigation safety and guide storm waters through the inlet, the U.S. Army Corps of Engineers (USACE) is investigating the rehabilitation and redesign of jetties using numerical and physical modeling of storm waves. This paper is focused on numerical wave modeling of the existing jetties and providing input forcing information to physical model and redesign of jetties.

NUMERICAL MODELS

The Coastal Modeling System (CMS; Demirebelik and Rosati 2011) developed at ERDC was applied for wave estimates around the jetty structures in the present study. The CMS is a suite of hydrodynamics, wave, and sediment transport models including CMS-Wave and CMS-Flow. CMS-Wave is a full-plane spectral wave transformation model that solves the steady-state (time-independent) wave-action balance diffraction equation (Lin et al. 2008, 2011) to simulate surface wave diffraction, refraction, reflection, wave breaking and dissipation mechanisms, wave-wave and wave-current interactions, and wave generation and growth. The model can run faster in a half-plane mode such that primary waves propagate and transform only from the seaward boundary toward shore. Additional features include the grid nesting capability, variable rectangle cells, wave run-up on beach face, wave transmission through structures, and wave overtopping. CMS-Flow is a hydrodynamic and sediment transport model capable of simulating depth-averaged circulation and sediment transport forced by tides, wind, river inflow, and waves (Buttolph et al. 2006). The hydrodynamic model solves the conservative form of shallow water equations by finite volume method and includes terms for the Coriolis force, wind stress, wave stress, bottom friction, and turbulent diffusion.

CMS-Wave and CMS-Flow can be run separately or coupled on a non-uniform Cartesian grid. In the coupling mode, the variables passed from CMS-Wave to CMS-Flow are the significant wave height, spectral peak wave period, mean wave direction, wave breaking dissipation, and radiation stress gradients. CMS-Wave uses the update bathymetry, water levels, and currents from CMS-Flow. The coupling can be operated through the Surface-water Modeling System (SMS, Zundel, 2006) by providing the total simulation period of CMS-Flow with constant interval of running CMS-Wave. Coupling CMS-Flow and CMS-Wave can simulate many important short-term to long-term processes like the shoreline change, channel infilling, breaching to shore and damage to coastal structure, and storm-induced flooding and erosion. Both models have the nested grid capability as an alternative for circulation, sediment calculation, and wave transformation in the local higher resolution area.

METHODOLOGY

Numerical wave modeling in this study consisted of three parts: (1) analysis of offshore wave climate based on field measurements and long-term hindcasting information, (2) transformation of a combination of wave and water level conditions from offshore location to the project site, and (3)

¹ Coastal and Hydraulics Laboratory, U.S. Army Engineer Research and Development Center, 3909 Halls Ferry Road, Vicksburg, Mississippi, 39180, USA

transformation of waves for 20 most severe historical storms from offshore location to project site. The first part involved analysis of buoy/gauge data and long-term hindcasting database of offshore wave conditions from the USACE Wave Information Studies (WIS). The second part included the application of CMS-Wave to transform offshore wave climate conditions to project site. The third part included transformation of offshore waves interacting with water levels and currents to Coos Bay Inlet for 20 most severe historical storms.

A nested grid system consisting of two grids were used in the CMS simulations: (1) a parent grid with coarser resolution covering the regional area, and (2) a child grid representing the local Coos Bay Inlet area with finer resolution (Figure 1). Wave and current interactions were simulated by coupling of CMS-Wave and CMS-Flow to capture wave shoaling, reflection, and diffraction over strong tidal currents at the inlet. The parent grid simulation was driven by directional spectra and water levels specified along the open water boundaries and with surface wind forcing over the model domain. The parent grid model results, including water levels, currents and wave spectra, were used as input to the child grid. Wave model results were saved in the child grid at 355 output locations along 21 transects (Figure 2) to quantify wave properties for input to physical model and redesign of jetty structures.

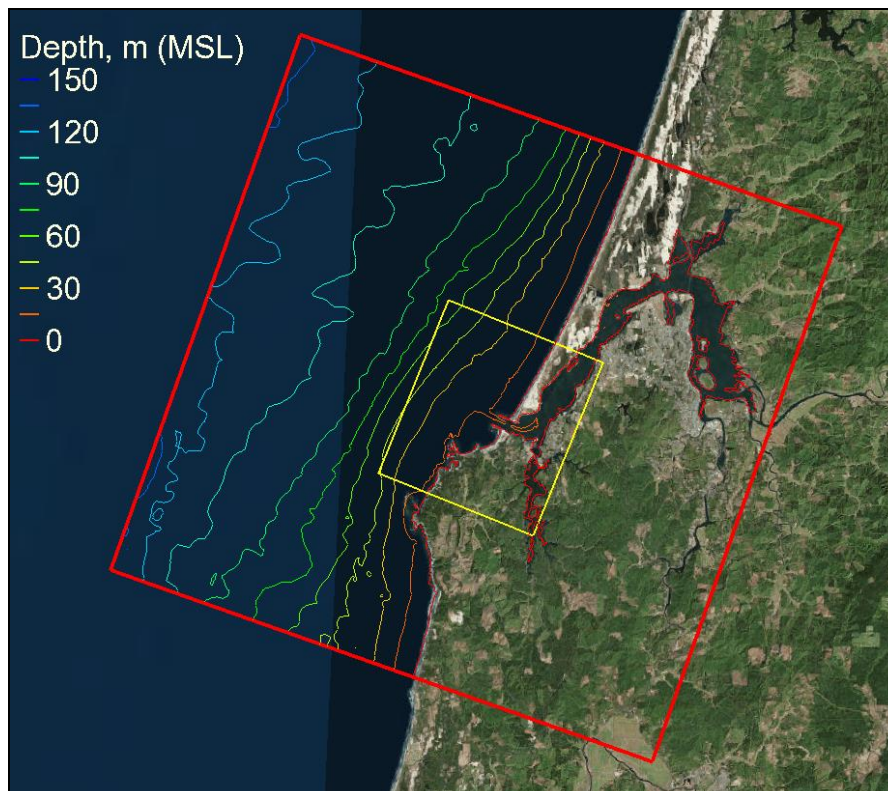


Figure 1. Parent grid domain (red box) and child grid domain (yellow box).

COASTAL WIND WAVE, WATER LEVEL, AND BATHYMETRY DATA

Field wave measurements outside Coos Bay are available from three locations: (1) a NDBC Buoy 46015 (<http://www.ndbc.noaa.gov/>) located 40 mi south of Coos Bay, (2) a CDIP Buoy 46229 (<https://cdip.ucsd.edu/>) 30 mi north of Coos Bay, and (3) an AWAC (Acoustic Waves and Currents) sensor located nearshore north of the Coos Bay inlet. The USACE Wave Information Studies (WIS) provided long-term Pacific coast hindcasting at 1-hr interval from 1980 through 2015 (36-year data). Water level data are available from AWAC sensor and NOAA Coastal Stations 9432780 (CHAO3), located inside the inlet at Charleston, OR, and 9431647 (PORO3) at Port Orford, OR. Figure 3 shows the location of NOAA CHAO3, NOAA PORO3, NDBC 46015, CDIP 46229, the nearshore AWAC sensor, and three WIS stations 83031, 83032, and 83033. Table 1 lists the locations and data duration of these coastal data stations. While Buoys 46015 and 46229 have collected directional wave data for approximately ten years, the nearshore AWAC has only two-month data from 18 September to 20 November 2015. Wind data are available from NDBC 46015, NOAA CHAO3, and NOAA PORO3.

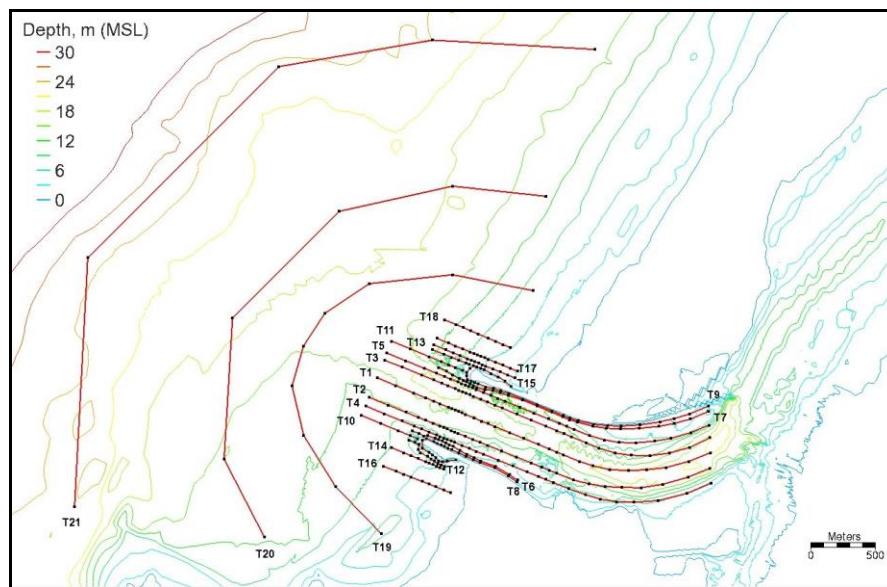


Figure 2. Child grid output locations along 21 transects (T1 to T21).

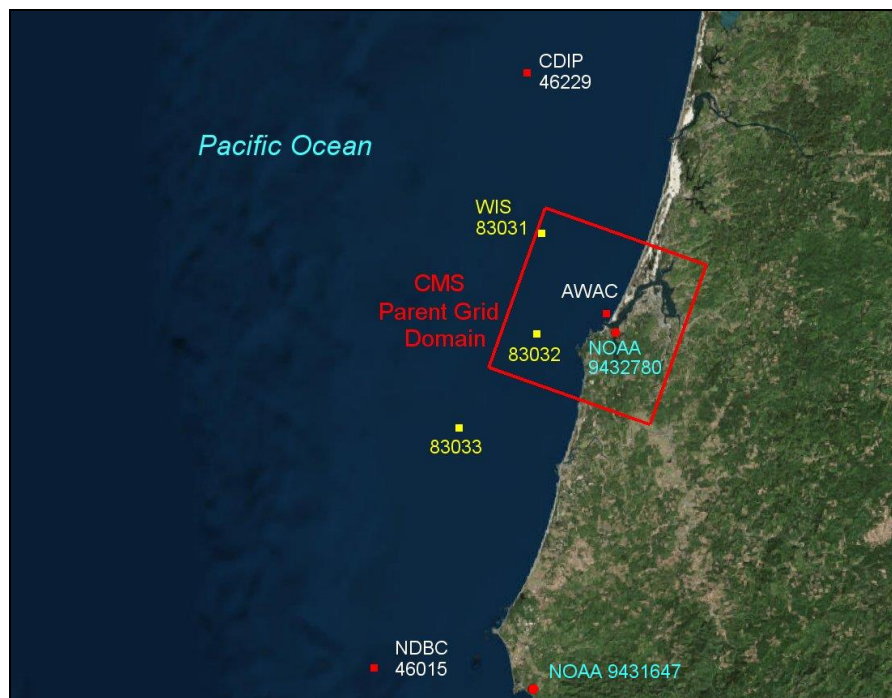


Figure 3. Location map of WIS and coastal gauging stations near Coos Bay.

Figure 4 shows the example of comparison of hindcasting waves from WIS 83032 and buoy data from NDBC 46015 and CDIP 46229 for October to December, 2010. Buoy data show very similar wave heights, periods, and directions between NDBC 46015 and CDIP 46229. Waves at CDIP 46229 turn a little more towards shore than at NDBC 46015 as a result of slightly stronger wave refraction at CDIP 46229 with shallower depth than NDBC 46015. The WIS 83032 hindcasting may occasionally overestimate or underestimate wave heights. Overall, wave hindcasting results from WIS 83032 are in good agreement with the field wave data. Figure 5 compares wave data collected at NDBC 46015, CDIP 46229, and AWAC sensor for September to November, 2015. Waves at AWAC turn more towards the shore than NDBC 46015 and CDIP 46229 as the wave refraction is stronger at AWAC sensor because of shallower depth. Wave height at AWAC sensor is generally smaller than at CDIP 46229 as a result of stronger wave energy dissipation from the bottom frictional loss.

Table 1. Coordinates, depth, and data length of WIS and coastal gauging stations.

Station	Latitude	Longitude	Nominal Depth	Data Length
WIS 83031	43.5° N	124.5° W	156 m	1980 – 2015*
WIS 83032	43.333° N	124.5° W	103 m	1980 – 2015*
WIS 83033	43.17° N	124.666° W	272 m	1980 – 2015*
NDBC 46015	42.764° N	124.832° W	420 m	2007 – 2018*
CDIP 46229	43.766° N	124.551° W	182 m	2008 – 2018*
AWAC	43.372° N	124.342° W	14 m	Sep - Nov,
NOAA 9432780	43.345° N	124.322° W	3 m	1996 – 2018**
NOAA 9431647	42.738° N	124.498° W	3 m	1996 – 2018**

* Directional wave data, ** Hourly water level data.

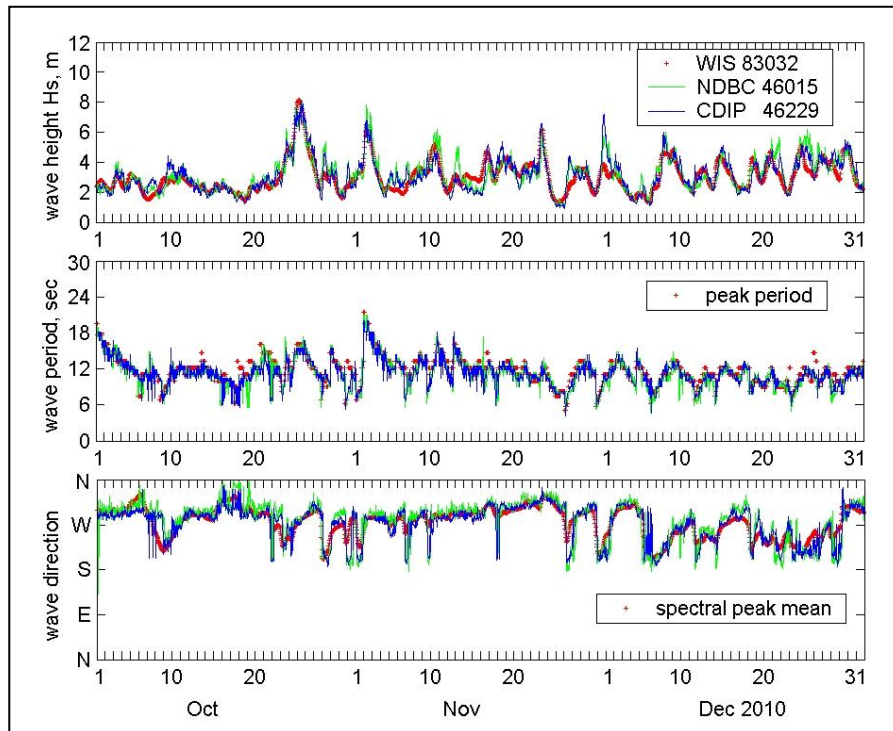
**Figure 4. Comparison of WIS 83032, NDBC 46015, and CDIP 46022 for Oct-Dec 2010.**

Figure 6 shows the wave roses at CDIP 46229, WIS 83032, and AWAC sensor for 18 September to 20 November, 2015, when the AWAC data are available. Note that wave rose for NDBC 46015 is not shown in the figure because of many missing wave data in November 2015. Figure 6 clearly shows smaller wave height and stronger diffraction at the AWAC sensor than at CDIP 46229 and WIS 83032.

Bathymetric data used for the CMS-Wave grids come mainly from five sources: (1) sonar measurements conducted by Oregon State University for the Coos Bay in 2014 (Wood and Ruggiero 2015), (2) a Lidar survey made by the Joint Airborne Lidar Bathymetry Technical Center of Expertise (JALBTCX) in 2014, (3) Coos Bay dredging placement site and inlet entrance channel surveys by the USACE Seattle District (NWP) in 2014 and 2015, (4) Inlet channel and jetty survey supported and completed by NWP in 2017, and (5) Coastal Digital Elevation Models (DEM) maintained by the National Geophysical Data Center (NGDC).

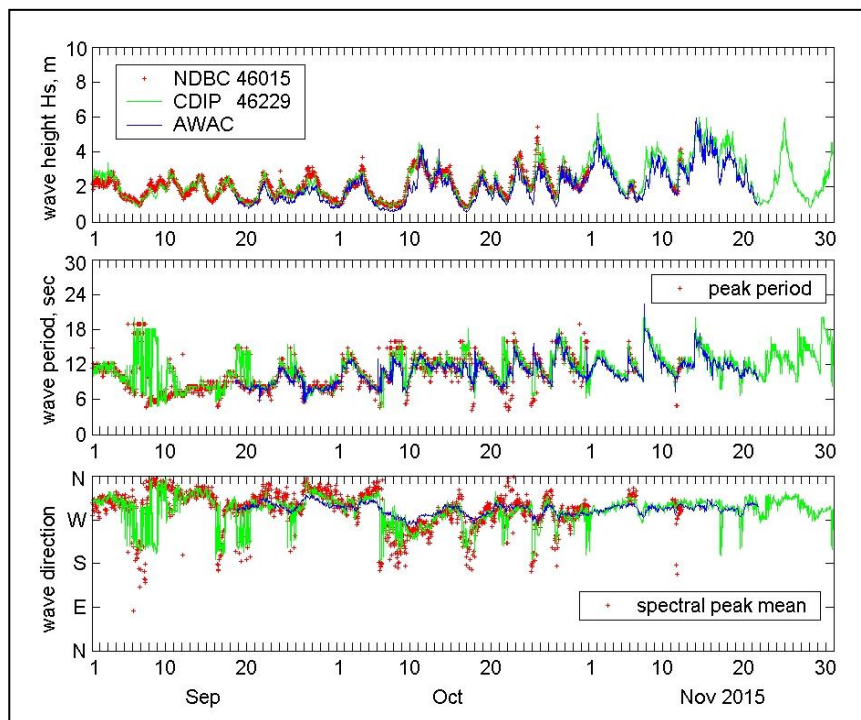


Figure 5. Comparison of NDBC 46015, CDIP 4622, and AWAC waves for Sep-Nov 2015.

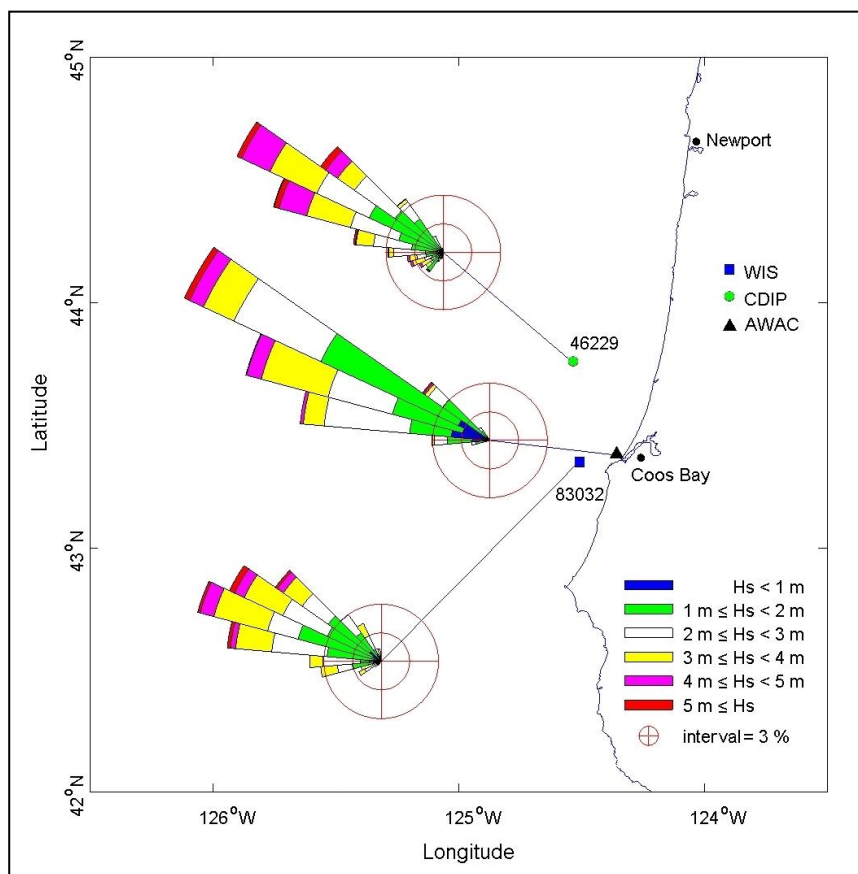


Figure 6. Wave rose comparison for 18 September to 20 November, 2015.

MODEL SETTINGS AND CALIBRATION

CMS-Wave was used to transform offshore waves from either WIS 83032 or coastal buoys to the project site. Wave modeling was performed using a parent grid covering the larger coastal bay region and a child grid covering the nearshore inlet area (Figure 1). Incident wave spectra were specified at the seaward boundary of the parent grid. The parent grid model results were saved along the open boundary of the child grid and used as input wave conditions to the child grid. The parent grid covers a square domain of approximately 32 km x 32 km including Coos Bay and extending offshore to the 150-m depth contour. It consists of 410 x 520 cells with varying size from 20 m to 320 m. Larger cells are used in deeper water and smaller cells in near-shore and inlet areas of the grid domain. The child grid is a subdomain of the parent grid. It is approximately 9.2 km x 10.3 km to cover the inlet, lower bay, and adjacent shoreline outside the bay. The child grid consists of 560 x 700 cells with varying size from 4 m in the in-let to around 100 m at four corners of the grid.

CMS-Wave were calibrated in the parent grid for the period of 18 September to 21 November, 2015. CMS-Wave was run in the half-plane mode using the incident waves from CDIP 46229 and model result was validated with the nearshore AWAC sensor. The modeling included wave refraction, diffraction (with the default diffraction intensity parameter = 4), and bottom friction (with the Darcy-Weisbach coefficient = 0.001). Wave breaking due to depth limitation is based on the extended Goda formula. The model forcing includes conditions with and without water level input, with and without wind forcing, and with interactions between waves and circulation. Table 2 presents the input conditions for model calibration.

Table 2. CMS-Wave calibration for 18 September – 21 November, 2015.

Condition	CMS-Wave	Water Level Input	Wind Forcing	With Circulation*
1	X			
2	X	X		
3	X		X	
4	X	X	X	
5	X	X		X
6	X	X	X	X
* Coupling CMS-Wave and CMS-Flow.				

The incident wave input is based on directional wave spectra measured from CDIP 46229. The water level input to CMS-Wave is based on data collected at NOAA Station 9432780 (CHAO3) at Charleston, OR (Figure 3). Wind forcing input is based on data from NDBC Buoy 46015. Figure 7 shows hourly wind measurements from NDBC 46015, and NOAA Stations CHAO3 and PORO3 for September to November, 2015.

The model wave interaction with flow circulation was performed by coupling CMS-Wave and CMS-Flow models (Lin et al. 2012). For the Coos Bay application, CMS-Flow has been calibrated in the previous study using current data collected in the upper bay and at the inlet entrance (Li et al. 2018). In the present study, CMS-Wave and CMS-Flow were run on the same model grids at 2-hr interval. The coupling of CMS-Wave and CMS-Flow is steered under a Surface-water Modeling System, SMS (Zundel, 2006). Figure 8 shows comparison of wave model results with wave-current and water level interaction with and without wind forcing input (Conditions 5 and 6) versus data at the AWAC sensor. The correlation of model significant heights (H_s) and AWAC data is high, with correlation coefficient great than 0.97. Model peak periods (T_p) also correlate well with AWAC data; the correlation coefficient is around 0.9. The absolute bias of model mean wave direction (θ_m) versus AWAC data is less than 6 deg. Tables 3 and 4 compare the bias and root-mean-square error (rmse) of model wave heights, periods, and directions versus AWAC data. CMS-Wave tends to slightly overestimate wave height and period (positive bias) in all 6 calibration conditions. While model results of Conditions 1 and 2 show smaller bias for mean wave period estimates, Conditions 3 and 4 provide smaller bias for mean wave height estimates. For the model maximum wave height, Conditions 5 and 6 yield smaller bias and rmse while Condition 6 yields the smallest bias. Figure 9 shows model water levels versus AWAC data for Condition 6. The CMS estimates well water levels in the calibration.

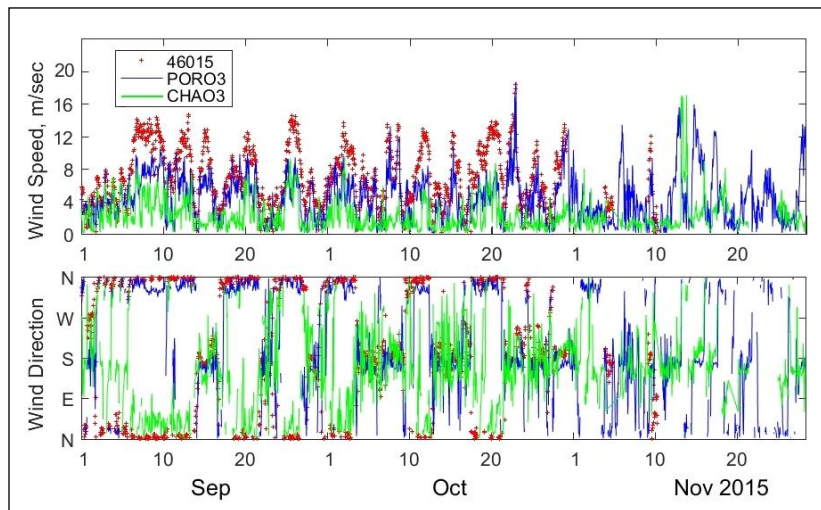


Figure 7. Comparison of NDBC 46015, NOAA CHAO3 and PORO3 winds for Sep-Nov 2015.

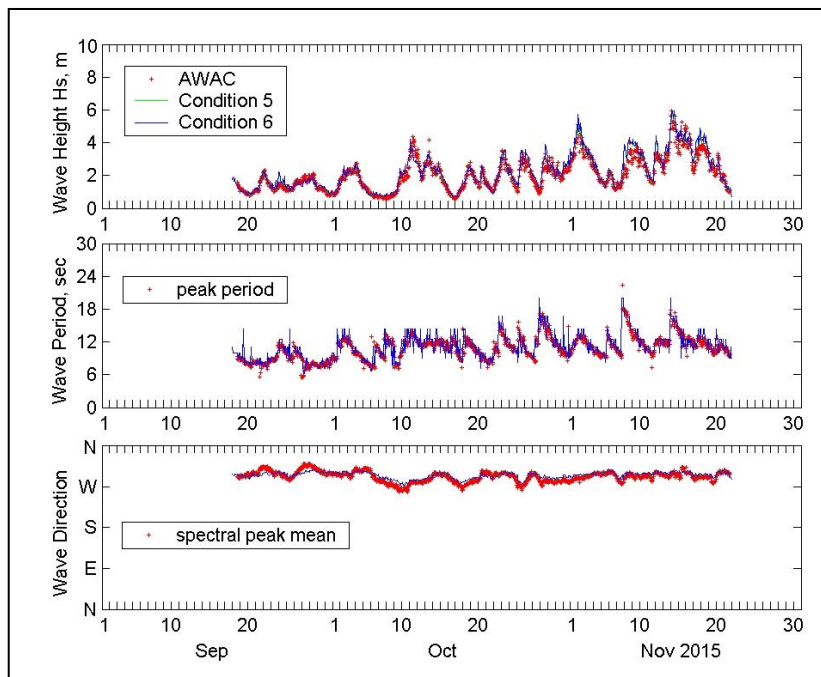


Figure 8. Model wave results for Conditions 5 and 6 versus AWAC data.

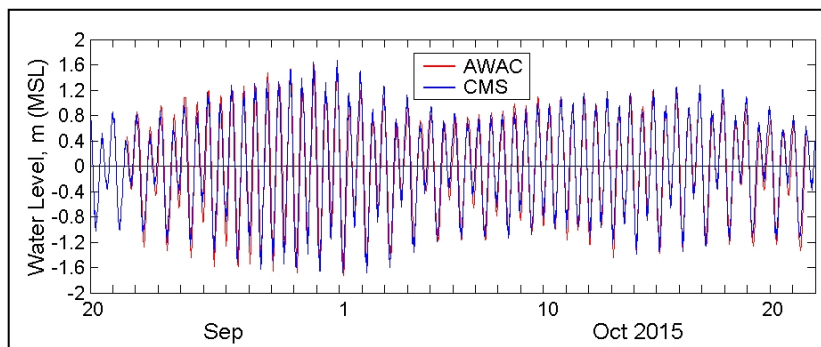


Figure 9. Model water level results for Condition 6 versus AWAC data.

Table 3. Statistics of model wave heights versus AWAC data.

Validation Condition	$H_{s,mean}$ (m)	$H_{s,bias}^*$ (m)	$H_{s,max}$ (m)	$H_{s,max,bias}^*$ (m)	$H_{s,rmse}$ (m)
1	2.17	0.07	5.82	-0.13	0.24
2	2.17	0.07	5.79	-0.16	0.24
3	2.13	0.03	5.56	-0.39	0.23
4	2.13	0.03	5.57	-0.38	0.23
5	2.19	0.09	5.87	-0.08	0.22
6	2.21	0.11	5.96	0.01	0.23
* Bias = mean(model calc.- data) mean($H_{s,AWAC}$) = 2.1 m; max($H_{s,AWAC}$) = 5.95 m					

Table 4. Statistics of model wave periods and directions versus AWAC data.

Validation Condition	$T_{p,mean}$ (sec)	$T_{p,bias}^*$ (sec)	$T_{p,rmse}$ (sec)	$ \theta_{m,bias} ^{**}$ (deg)	$\theta_{m,rmse}$ (deg)
1	11.2	0.25	1.08	3.4	7.4
2	11.2	0.25	1.08	3.4	7.4
3	11.3	0.32	1.09	4.2	8.4
4	11.3	0.32	1.08	4.2	8.4
5	11.2	0.27	1.07	3.1	7.4
6	11.2	0.27	1.07	3.2	7.4
* Bias = mean(model calc.- data) mean ($T_{p,AWAC}$) = 10.9 sec ** $ \theta_{m,bias} $ is the absolute bias of mean model wave direction; $\theta_{m,AWAC}$ = 292 deg					

TRANSFORMATION OF OFFSHORE SYNTHETIC WAVE CONDITIONS TO NEARSHORE

Based on the long-term wave hindcasting data from WIS 83032 offshore Coos Bay and water level measurements from NOAA Station CHAO3 inside the inlet, a combination of twelve (12) incident wave heights, eight (8) peak periods, and five (5) mean wave directions with nine (9) water levels was used as offshore boundary conditions, a total of 4320 (12 x 8 x 5 x 9) simulations, for wave transformation to Coos Bay. Table 5 presents the combination of offshore incident wave forcing parameters and values for CMS-Wave boundary conditions.

Table 5. Offshore incident wave combinations.

Offshore Wave Forcing Parameters	Increments
Significant Height (m)	1, 3, 5, 7, 8, 9, 10, 11, 12, 13, 14, 15
Peak Period (sec)	8, 10, 12, 14, 16, 18, 20, 22
Mean Direction (deg, meteorological)	220, 250, 280, 310, 340
Water Level, MSL (m)	-1.5, -1, -0.5, 0, 0.5, 1, 1.5, 2, 2.5

The wave transformation from offshore to Coos Bay nearshore was conducted on parent and child grids. Incident wave spectra were made with 35 directional bins in a half-plane mode (with a 5-deg bin resolution) and 30 frequency bins (0.04 to 0.33 Hz, with a 0.01-Hz increment). Input spectra were given as of narrower frequency band (spectral peak enhancement factor = 4) and with narrow directional range (directional spreading parameter = 20). Wave modeling included wave shoaling, refraction, diffraction, reflection along jetties (reflection coefficient = 0.3), bottom friction, and wave runup processes. Wind input and wave-current interaction were not included in the simulation. Model wave results from the child grid were extracted along 21 transects (T1 to T21) with 355 save locations on these transects (Figure 2). Figure 10 shows the example of model wave heights along Transect T9 (around North Jetty) from Save Stations 218 (outside inlet) to 250 (inside inlet) under the incident significant wave of 12 m (a 50-year life cycle), 20 sec, and 310 deg (from NW) for water level (WL) input of 0 m, 0.5 m, 1.0 m, 1.5 m, 2.0 m, and 2.5 m. The effect of future sea level rise on wave heights along North Jetty is much greater outside the inlet than inside the inlet.

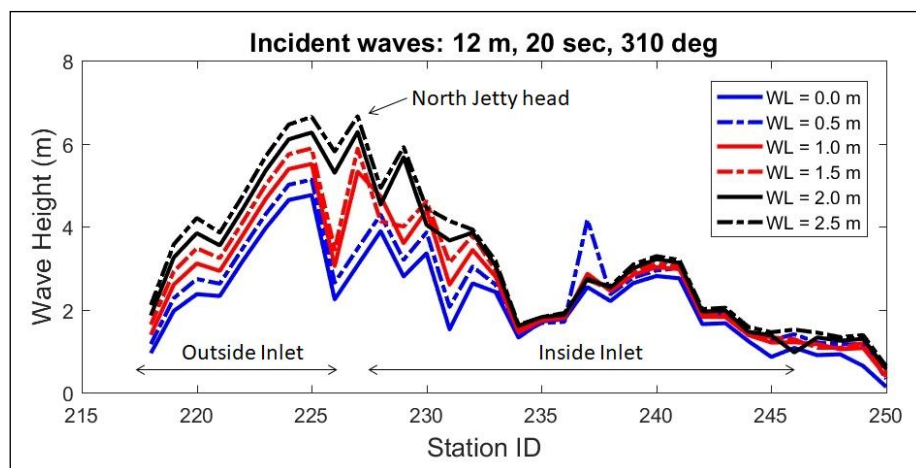


Figure 10. Model wave heights under incident waves of 12 m, 20 sec, 310 deg and different water level input around North Jetty along Transect T9.

TRANSFORMATION OF SEVERE STORM WAVES TO NEARSHORE

Transformation of historical storm waves from offshore to Coos Bay was conducted for top 20 storm conditions based on hindcasting data from WIS 83032 (see Table 6). CMS-Wave and CMS-Flow were coupled on the parent and child grids at 1-hr interval to include wave-current interactions. The water level input to the CMS is based on long-term data collected at NOAA Coastal Station 9432780 (CHAO3). Figure 11 shows, for example, the water level data from NOAA Coastal Station 9432780 corresponding to No. 1 Storm listed in Table 6. Wind forcing is based on the hindcasting data from WIS 83032. Figure 12 shows wind and wave hindcasting data from WIS 83032 for the No.1 Storm. Maximum significant waves reach to approximately 11 m and 18 sec with 21 m/sec wind speed. Wave reflection and wave runup on jetties were included in the simulation.

Figures 13 and 14 show model wave height fields under the maximum incident wave input on parent and child grids, respectively, for the No. 1 Storm condition. Model results show clearly wave shoaling along inlet channel south shoreline, wave dissipation adjacent to the inlet entrance, refraction outside the inlet, wave diffraction at inlet jetties, and waves entering the inlet navigation channel. Figures 15 and 16 show model maximum flood and ebb current fields, respectively, around peak hours of the storm. The ebb current at the inlet entrance is greater with relatively lower water level than the flood current magnitude with higher water level. The depth-averaged current magnitude at inlet channel during maximum flood and ebb conditions is greater than 2 m/sec. The strong current at inlet mouth and navigation channel can greatly affect wave height, period, and direction around jetties.

Figure 17 show model wave heights corresponding to maximum incident wave for the No. 1 Storm condition along Transects T1 to T5 (Figure 2) between north and south jetties. Waves dissipate the energy quickly from outside inlet mouth to inside and backside of the inlet. The variation of wave height across channel from T1 to T5 is, however, quite significant as a result of strong local wave, current, and structure interactions.

Table 6. Top 20 storms ranked by wave height for WIS 83032 (1980-2015).

Rank	Start Timestamp*	End Timestamp*	Peak Timestamp*	$H_{s,max}^{**}$ (m)	T_p^{**} (sec)	θ_m^{**} (deg)	Duration (hrs)
1	2008010414	2008010609	2008010508	10.97	18.34	256	43
2	1981111403	1981111506	1981111414	10.82	15.47	243	27
3	1995121208	1995121516	1995121302	10.55	16.09	248	80
4	1999102802	1999102909	1999102814	10.39	18.1	263	31
5	2001111918	2001112307	2001112213	9.19	15.63	261	85
6	2000122202	2000122304	2000122210	9.04	17.25	255	27
7	2007120216	2007120509	2007120319	8.92	14.59	220	68
8	1982121416	1982121915	1982121615	8.65	16.21	255	120
9	1998112312	1998112706	1998112411	8.63	15.88	264	90
10	1987113020	1987120317	1987120206	8.32	17.33	270	70
11	2015121000	2015121212	2015121100	8.91	16.96	270	60
12	2014011115	2014011220	2014011205	8.67	16.06	285	29
13	2006121308	2006121604	2006121507	8.3	14.46	264	68
14	2001121318	2001121504	2001121407	8.29	13.28	288	34
15	2006020406	2006020513	2006020415	8.25	14.48	260	31
16	2002121411	2002121801	2002121600	8.17	14.51	239	86
17	1983012405	1983012800	1983012622	8.15	19.94	250	91
18	1999030300	1999030403	1999030308	8.13	13.31	236	27
19	2010102415	2010102610	2010102508	8.12	16.05	278	43
20	1984022409	1984022517	1984022501	8.07	15.81	280	32

* 10-digit timestamp in "yyyymmddhh": yyyy for year, mm for month, dd for day, and hh for hr (GMT)

** $H_{s,max}$, T_p , and θ_m corresponding to storm peak wave height condition

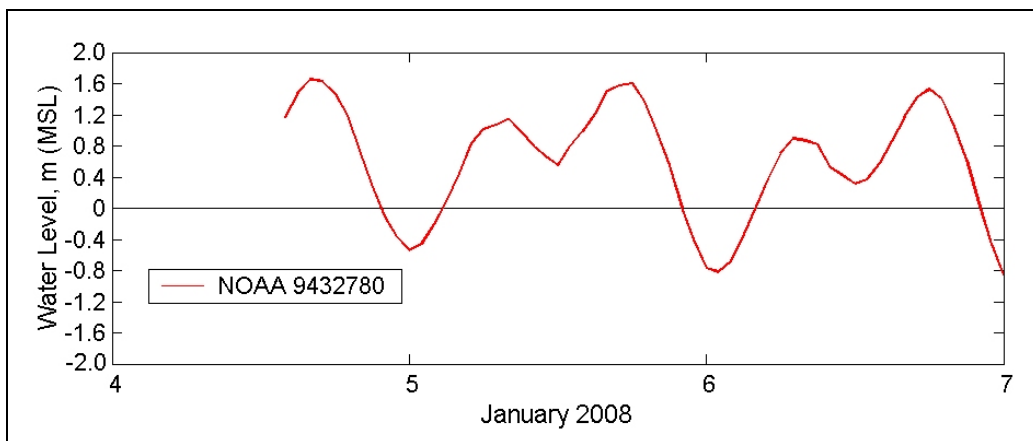


Figure 11. Water level data for No. 1 Storm at NOAA Station 9432780.

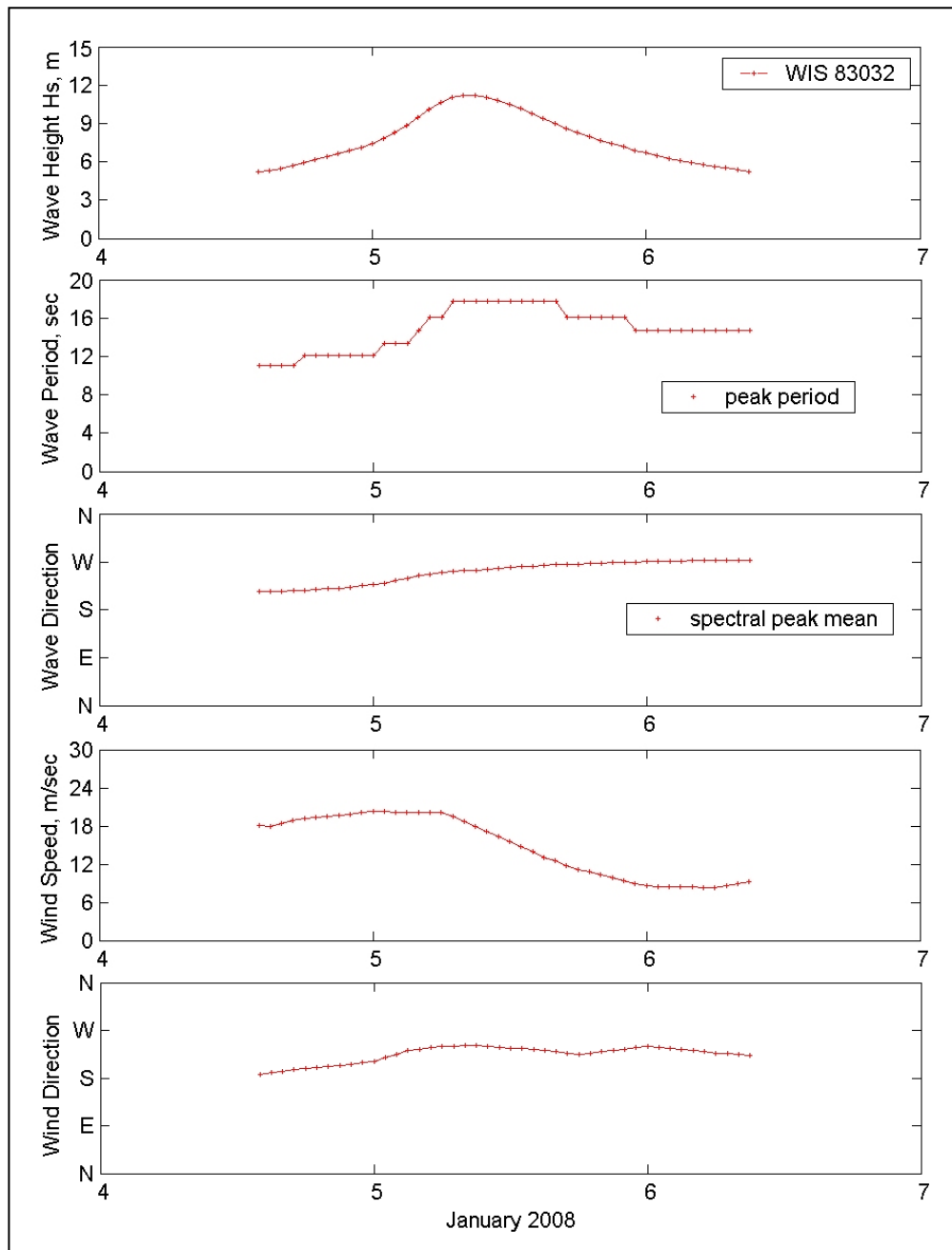


Figure 12. Hindcasting wind and wave data for No. 1 Storm at WIS 83032.

Model wave results were used in the physical model study conducted at the USACE Coastal and Hydraulics Laboratory (CHL). The physical model (scale at 1:55) covers the inlet area from approximately 20-m depth contour (MSL) offshore to the backside of the inlet. Model results from the child grid Save Station 347 outside the inlet in the middle of Transect T20 were used for the incident wave in the physical model. Figure 18 shows the model maximum wave spectrum ($\text{m}^2\text{sec/radian}$) at the child grid Save Station 347 corresponding to No.1 Storm in WIS 83032. The wave height, peak period, and mean direction associated with this spectrum are 8.78 m, 17 sec, and 270 deg (due west), respectively. This wave spectrum approximately corresponds to the maximum wave condition in the 4-year life cycle event. Water levels were included while the tidal current in or out of the inlet was not simulated in the physical model.

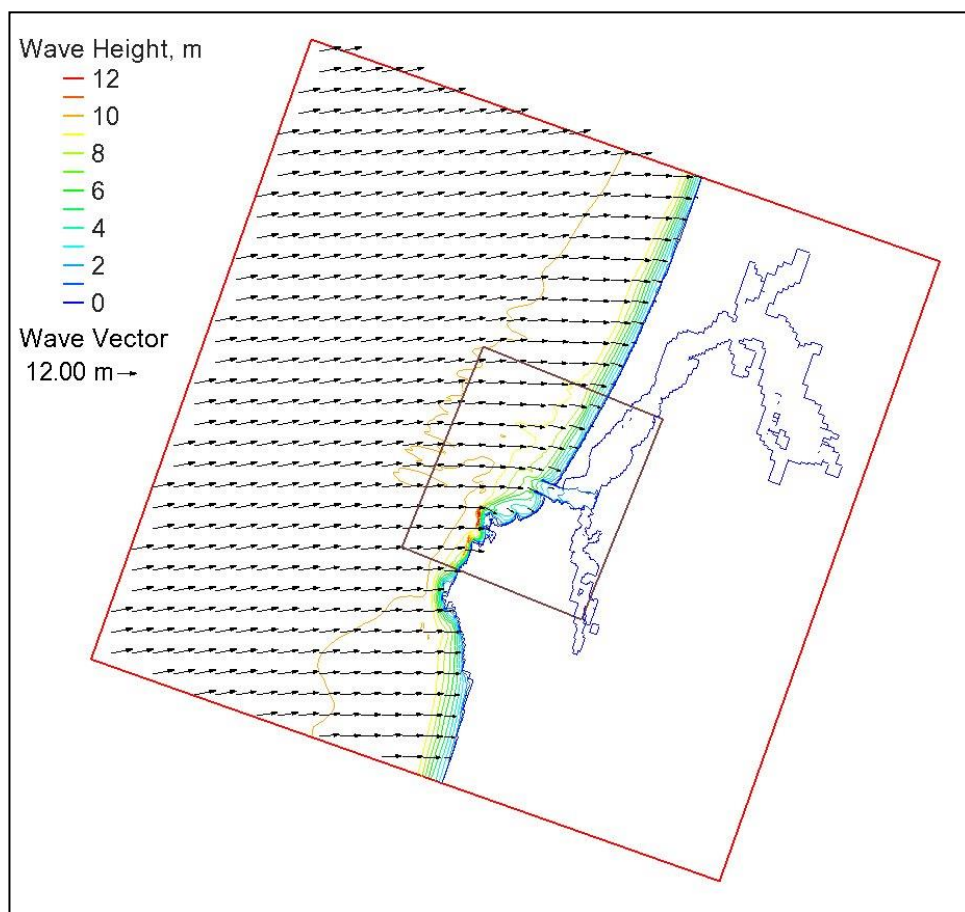


Figure 13. Maximum wave height field on the parent grid for No. 1 Storm from WIS 83032.

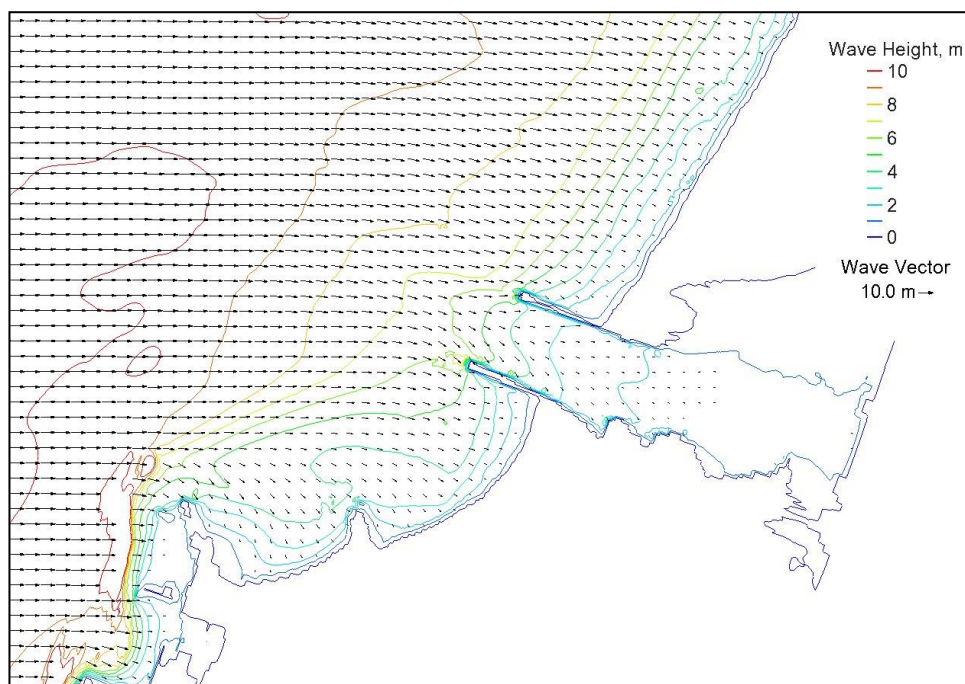


Figure 14. Maximum wave height field on the child grid for No. 1 Storm from WIS 83032.

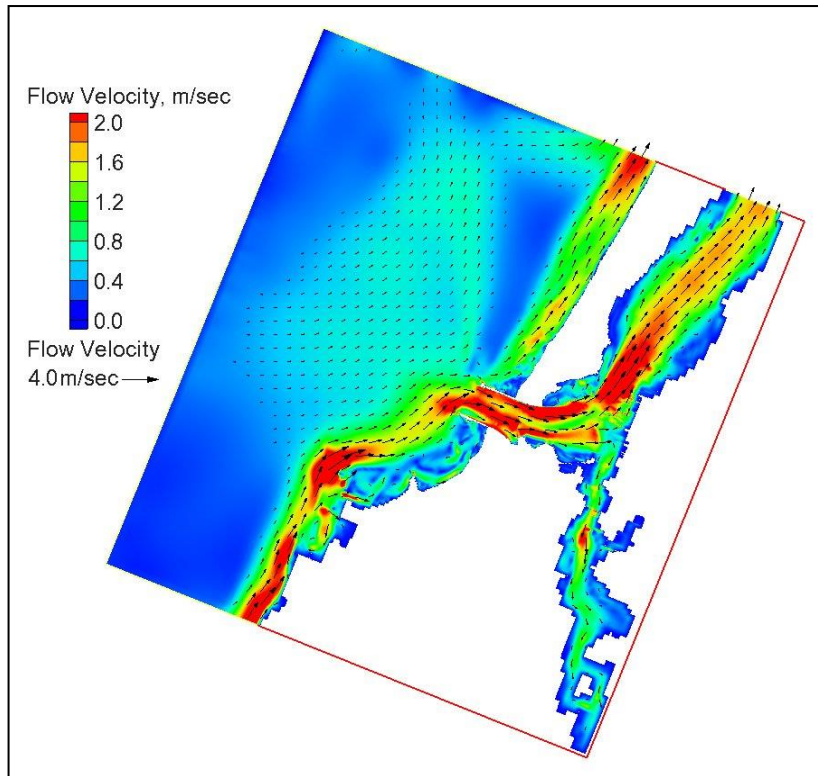


Figure 15. Model maximum flood current field for No. 1 Storm from WIS 83032.

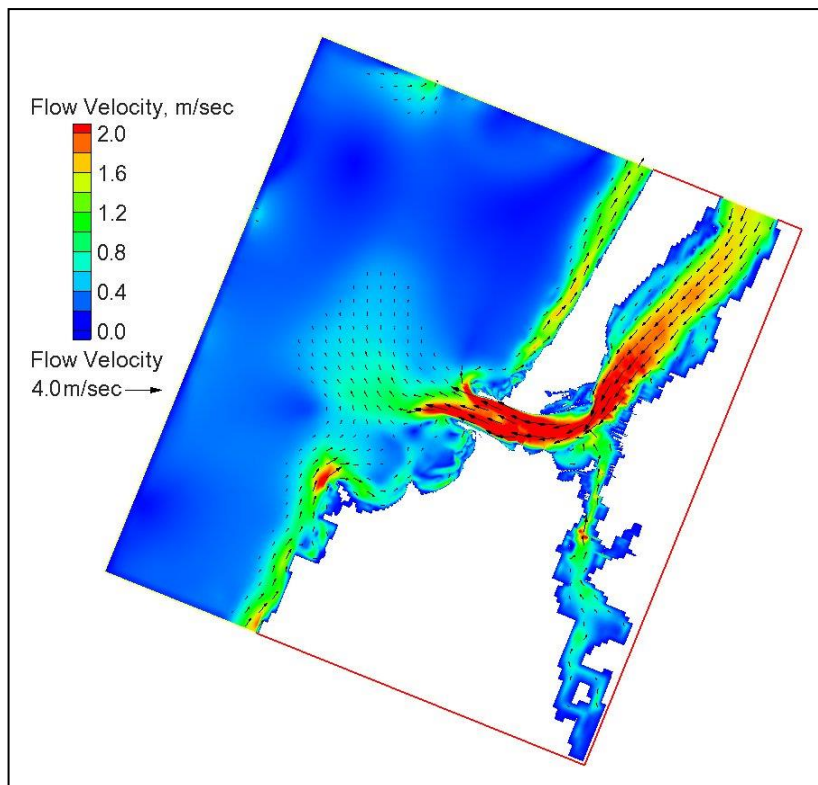


Figure 16. Model maximum ebb current field for No. 1 Storm from WIS 83032.

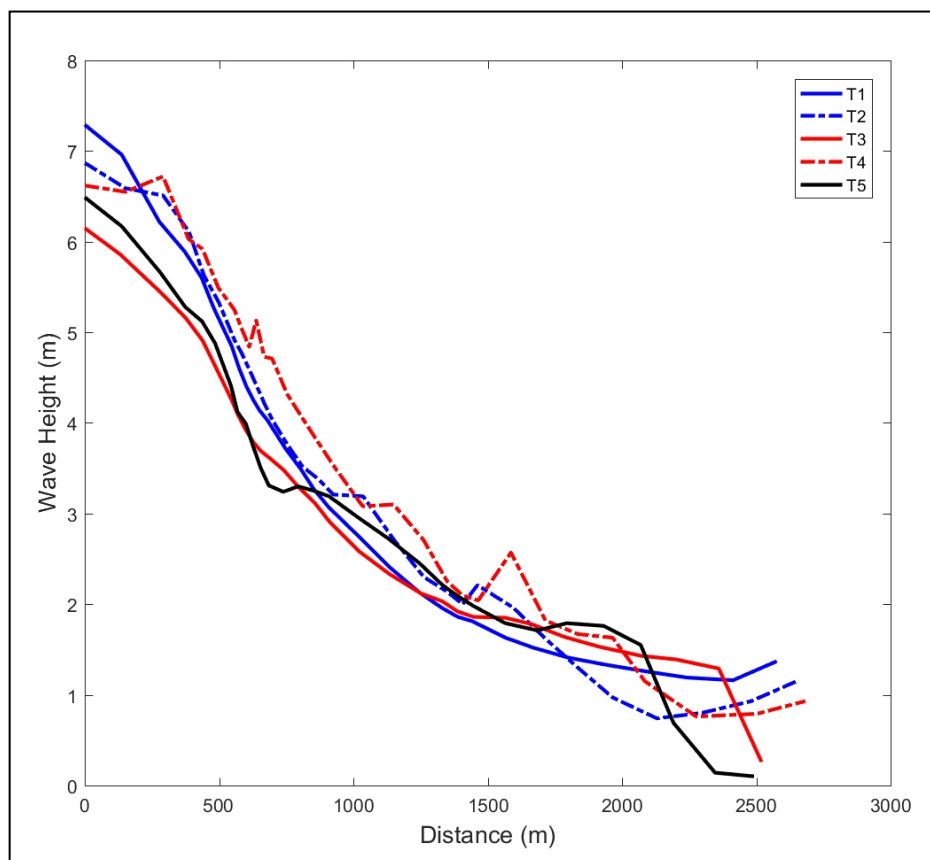


Figure 17. Model maximum wave heights along T1 to T5 between inlet jetties.

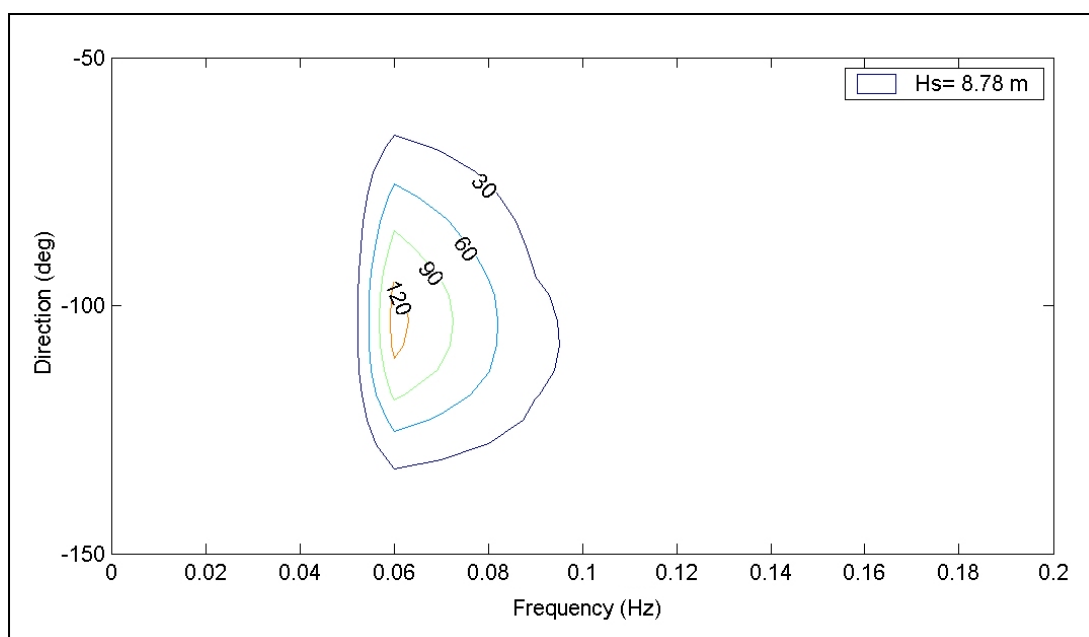


Figure 18. Model maximum wave spectrum at child grid Save Station 347 for No.1 Storm.

CONCLUSIONS

A numerical wave spectral model CMS-Wave is used in the investigation of jetty repair and rehabilitation at Coos Bay Inlet, Oregon. The input to the model includes field measurements of wind, waves, water levels, and long-term wave hindcasting database from the WIS. CMS-Wave was validated with high correlation (> 0.9) to wave height, period, and direction data collected at the nearshore AWAC sensor outside the inlet. The model wave interaction with flow circulation was performed by coupling CMS-Wave and a hydrodynamic model CMS-Flow on the same grid system. Model simulations with the interaction of wave and current produce more satisfactory results as the current in the Coos Bay Inlet is usually strong (depth-averaged current magnitude > 2 m/sec) affecting waves at and around the entrance channel. Model storm results show clearly wave shoaling along inlet channel south shoreline, wave dissipation adjacent to the inlet entrance, refraction outside the inlet, wave diffraction at inlet jetties, and wave energy propagating into the inlet navigation channel.

Transformation of offshore waves to Coos Bay was conducted for a combination of 12 significant heights, 8 peak periods, 5 mean wave directions, and 9 water levels, as well as the top 20 historical storms in the WIS Station 83032 data source. The effect of future sea level rise (higher water level) on wave heights along North Jetty is much greater outside the inlet than inside the inlet. The present numerical model results were analyzed and used for supplying input wave information to evaluation of jetty repair and redesign in the physical model.

ACKNOWLEDGMENTS

The authors are grateful to Dr. Julie D. Rosati for continual support and encouragement towards development and improvement of wave estimate capabilities to increase the reliability and usefulness of numerical Coastal Modeling System. Permission was granted by the Chief, U.S. Army Corps of Engineers to publish this information.

REFERENCES

- Buttolph, A. M., C. W. Reed, N. C. Kraus, N. Ono, M. Larson, B. Camenen, H. Hanson, T. Wamsley, and A. K. Zundel. 2006. Two-dimensional depth-averaged circulation model CMS-M2D: Version 3.0, Report 2: Sediment transport and morphology change. Coastal and Hydraulics Laboratory Technical Report ERDC/CHL TR-06-7. Vicksburg, MS: U.S. Army Engineer Research and Development Center.
- Demirbilek, Z. and J. D. Rosati. 2011. Verification and validation of the Coastal Modeling System: Report I, Executive Summary. Technical Report ERDC/CHL-TR-11-10. Vicksburg, MS: U.S. Army Engineer Research and Development Center.
- Li, H., T. Lackey, T.M. Beck, H.R. Moritz, K. Groth, T. Puckette, and J. Marsh. 2018. Field measurements, sediment tracer study, and numerical modeling at Coos Bay Inlet, Oregon. ERDC/CHL TR-18-6. Vicksburg, MS: U.S. Army Engineer Research and Development Center.
- Lin, L., Z. Demirbilek, and H. Mase. 2011. Recent capabilities of CMS-Wave: A coastal wave model for inlets and navigation projects. Proceedings, Symposium to honor Dr. Nicholas Kraus. *Journal of Coastal Research*, Special Issue 59, 7-14.
- Lin, L. Z. Demirbilek, H. Mase, J. Zheng, and F. Yamada. 2008. *CMS-Wave: a nearshore spectral wave processes model for coastal inlets and navigation projects*. Coastal Inlets Research Program, Coastal and Hydraulics Laboratory Technical Report ERDC/CHL TR-08-13. Vicksburg, MS: U.S. Army Engineer Research and Development Center.
- Lin, L., J. Rosati III, and Z. Demirbilek. 2012. CMS-Wave model: Part 5. Full-plane wave transformation and grid nesting. ERDC/CHL CHETN-IV-81. Vicksburg, MS: U.S. Army Engineer Research and Development Center.
- Zundel, A. K. 2006. Surface-water Modeling System reference manual: Version 9.2. Provo, UT: Brigham Young University Environmental Modeling Research Laboratory.